

# Dynamic Simulation of an Induction-Motor Centrifugal-Pump System under Variable Speed Conditions

Xiwen Guo<sup>1,2,3</sup>, Yuliang Wu<sup>1,2</sup>, Guoli Li<sup>1,2,3</sup>, Chao Lu<sup>1,2</sup>

<sup>1</sup> School of Electrical Engineering and Automation, Anhui University, Hefei, Anhui, China

<sup>2</sup> National Engineering Laboratory of Energy-saving Motor & Control Technique, Anhui University, Hefei, Anhui, China

<sup>3</sup> Engineering Research Center of Power Quality, Ministry of Education, Anhui University, Hefei, Anhui, China  
E-mail: xwguo2008@126.com

**Abstract.** With the centrifugal pump widely used in the industry, the characteristics of its high efficiency and energy saving have gained more attention. It has a certain significance to analyze the efficiency of the pump unit in a model of the motor-pump system. In this paper, the efficiency of the centrifugal pump at a variable rotating speed is analyzed by using the vector control strategy. Firstly, the rotor-flux-oriented vector control strategy is used to control the induction motor. Secondly, a centrifugal pump model was built based on structural characteristics in SimHydraulics. Finally, a dynamic simulation of the motor-pump system was completed in MATLAB/Simulink under variable speed conditions. The simulation results show that the high-efficiency rate of the system is in the range from 2000r/min to 2500r/min.

**Keywords:** centrifugal pump, three-phase induction motor, vector control, variable speed control

## Dinamična simulacija indukcijske centrifugalne črpalke pri spremenljivi hitrosti delovanja

S široko uporabo industrijskih centrifugalnih črpalk se je pokazala tudi potreba po njihovem učinkovitem in varčnem delovanju. Posebna pozornost je namenjena učinkovitosti črpalne enote. V članku analiziramo učinkovitost centrifugalne črpalke z uporabo različnega vektorskega krmiljenja. Simulacijo delovanja črpalke smo izvedli v okolju MATLAB/Simulink pri spremenljivi hitrosti delovanja. Rezultati simulacij so pokazali, da je delovanje najučinkovitejše med 2000 vrt/min in 2500 vrt/min.

## 1. INTRODUCTION

The centrifugal pump has a good hydraulic performance, it suits for a small flow and large lift occasions, which in the industrial, agricultural and commercial are dominant. In practice, the pump is driven by the motor as a load. The efficiencies of the motor are generally able to reach more than 90%, and the pump efficiency can reach only 50%. So the energy efficiency in the motor-pump system is particularly important [1].

In order to improve the overall efficiency of the motor-pump system, it is necessary to reduce the power losses of the pump unit [2]. The efficiency of the pump is determined by its speed, flow and head characteristics. The traditional way is to adjust the rate of the flow through the valve of the pump to achieve the purpose of changing the efficiency and head of the pump. However, the control valve increase the liquid

resistance and friction coefficient in the pipeline, so that the valve consumes a part of the energy of the system. Currently, the speed can be adjusted to control the flow, which to achieve the controlling efficiency. The additional losses caused by the throttle valve are thus reduced [3]. Generally, the V/F constant pressure frequency ratio method is used to adjust the speed. The disadvantages of this method are open-loop control and poor dynamic response. The vector control assumes good stability, fast response and good accuracy to match the needs of the pump [4-5]. Therefore, this paper adopts the rotor field oriented vector control strategy to quickly match the speed of the pump.

The efficiency of the centrifugal pump under variable speed conditions is analyzed by controlling the rotor-field-oriented. It is of a great significance to further research how to improve the overall efficiency of the motor-pump system [6-7]. This paper consists of three main parts. A model of the rotor-flux-oriented vector control of induction motor is presented in Section 1. A model and characteristic analysis of the pump are shown in Section 2. Finally, the simulation results are analyzed in Section 3.

## 2. MODELING OF VECTOR CONTROL FOR THE INDUCTION MOTOR

In practical applications, the three-phase induction motors often need to control different speeds to meet the requirements of different loads. Therefore, it is very

important to establish a reasonable speed-control model of the induction motor. Particularly, the vector control system can meet these requirements without changing the performance of the motor, slip-vector control, air-gap magnetic-field-oriented vector control and rotor-flux-oriented vector control. The rotor-flux-oriented vector control enables a decoupled control of the torque and flux linkage, so that the torque does not affect the flux linkage.

In the motor-pump system, the vector control transforms the coordinate. The mathematical model of the induction motor in a two-phase stationary coordinate is converted into a mathematical model of a two-phase rotating coordinate. As the rotor of the squirrel-cage induction motor is short-circuited, the voltage equations of the induction motor in the rotating coordinate are expressed as follows:

$$\begin{bmatrix} u_{sd} \\ u_{sq} \\ 0 \\ 0 \end{bmatrix} = \begin{bmatrix} R_s + L_s p & -\omega_1 L_s & L_m p & -\omega_1 L_m \\ \omega_1 L_s & R_s + L_s p & \omega_1 L_m & L_m p \\ L_m p & -\omega_s L_m & R_r + L_r p & -\omega_s L_r \\ \omega_s L_m & L_m p & \omega_s L_r & R_r + L_r p \end{bmatrix} \begin{bmatrix} i_{sd} \\ i_{sq} \\ i_{rd} \\ i_{rq} \end{bmatrix} \quad (1)$$

The flux equation is obtained as follows:

$$\begin{bmatrix} \psi_{sd} \\ \psi_{sq} \\ \psi_{rd} \\ \psi_{rq} \end{bmatrix} = \begin{bmatrix} L_s & 0 & L_m & 0 \\ 0 & L_s & 0 & L_m \\ L_m & 0 & L_r & 0 \\ 0 & L_m & 0 & L_r \end{bmatrix} \begin{bmatrix} i_{sd} \\ i_{sq} \\ i_{rd} \\ i_{rq} \end{bmatrix} \quad (2)$$

The electromagnetic torque equation is obtained as follow:

$$T_e = T_L + \frac{J}{p_m} \frac{d\omega_r}{dt} = p_m L_m (i_{sq} i_{rd} - i_{sd} i_{rq}) \quad (3)$$

Where:

- $\omega_s$  ... the slip angle speed,
- $\omega_1$  ... the synchronous angular velocity,
- $\omega_r$  ... the rotor angular velocity,
- $u_{sd}$  ... the stator voltage on the d axis,
- $u_{sq}$  ... the stator voltage on the q axis,
- $u_{rd}$  ... the rotor voltage on the d axis,
- $u_{rq}$  ... the rotor voltage on the q axis,
- $i_{sd}$  ... the stator current on the d axis,
- $i_{sq}$  ... the stator current on the q axis,
- $i_{rd}$  ... the rotor current on the d axis,
- $i_{rq}$  ... the rotor current on the q axis,
- $\psi_{sd}$  ... the stator-flux-linkage on the d axis,
- $\psi_{sq}$  ... the stator-flux-linkage on the q axis,
- $\psi_{rd}$  ... the rotor-flux-linkage on the d axis,
- $\psi_{rq}$  ... the rotor-flux-linkage on the q axis,
- $p_m$  ... the number of the motor poles,
- $p$  ... the differential operator,
- $J$  ... the moment of inertia.

In the field-oriented vector-control system, the  $d-q$  coordinate system is generally placed in the induction rotating magnetic field. The AC quantity of the stationary coordinate system is converted into the DC quantity in the rotating coordinate system. The d axis is set to coincide with the rotor-flux linkage direction  $\psi_{rd} = \psi_r$ . The q axis is perpendicular to the direction of the rotor flux, and the component of rotor flux  $\psi_{rq}$  is zero. The rotor flux is generated by the d axis of the winding current. The voltage equations are:

$$\psi_r = \psi_{rd} = L_m i_{rd} + L_r i_{rd} \quad (4)$$

$$0 = \psi_{rq} = L_m i_{sq} + L_r i_{sq} \quad (5)$$

According to formulas (1), (2), (3) and (4):

$$T_e = T_L + \frac{J}{p_m} \frac{d\omega_r}{dt} = p_m L_m (i_{sq} i_{rd} - i_{sd} i_{rq}) = p_m \frac{L_m}{L_r} i_{sq} \psi_r \quad (6)$$

$$\psi_r = \psi_{rd} = \frac{L_m}{T_r p + 1} i_{sd} \quad (7)$$

Where:

- $T_r = \frac{L_r}{R_r}$  ... the rotor time constant.

It is well known that the flux and torque of the motor can be completely decoupled by the formulas (6) and (7). The electromagnetic torque is determined by the component on the q axis of the stator current and the rotor flux is determined by the component of the stator current on the d axis.

As rotor flux  $\psi_r$  is controlled by the stator current  $i_{sd}$ , the torque  $T_e$  is controlled by  $\psi_r$  and  $i_{sq}$ . So the following equation can be obtained:

$$i_{sd}^* = \frac{T_r p + 1}{L_m} \psi_r^* \quad (8)$$

$$i_{sq}^* = \frac{L_r}{p_m L_m} T_e^* \quad (9)$$

Where:

- $\psi_r^*$  ... expected value of the rotor flux,
- $T_e^*$  ... expected value of the torque,
- $i_{sd}^*$  ... excitation current of the stator,
- $i_{sq}^*$  ... torque current of the stator.

The process of the field-oriented vector-control strategy is shown in Fig. 1, where  $\psi_r$  is derived from the motor model. The speed controller ASR uses the PI control.

The calculated value of flux linkage  $\psi_r^*$  is 0.7Wb. The value is compared with the flux of the motor rotor, and the error regard as the input of the flux controller APR. According to the relation between the flux and excitation current, the excitation component of the stator current is  $i_{sd}^*$ . The flux and speed controller

are used to employ the PI controller to control the output. Taking into account the PI controller the saturation limits the output of the controller. The limiter limits of an external and internal limiter. The external limiter is set by the rated torque and the overload factor of the motor to control the output of the PI controller. The internal limiter maintains the output value at not less than the maximum value of the motor at a steady-state to control the output of the integrator. The parameters of the PI controller are calculated using the engineering experience method shown in Table 1.

Table 1: Parameters of the PI controller

Controller	$K_p$	Internal-limiter	$K_i$	External-limiter
ASR	10	-80~80	5	-80~80
APR	1.8	-15~15	100	-13~13

According to the motor model, the rotor-flux linkage vector position angle signal is  $\varphi = \int \omega_1 dt$ . The three-phase alternating current of the driving motor is obtained by the inverse transformation of the coordinate system and the inverter. Finally, the rotor-flux signal and the speed-signal output of the motor output are sent to the system as a feedback to produce the expected value of the torque and speed under a steady state. Simulation of the rotor-flux-oriented vector-control strategy system is shown in Fig. 2.

### 3. CENTRIFUGAL PUMP SYSTEM MODEL

The main parameters of the centrifugal pump include that the pump flow rate (Q), head (H), efficiency ( $\eta$ ) and speed (n). They are used as a criterion to measure the pump system and the main parameters for the dynamic model analysis. The analysis of the external characteristics of the centrifugal pump consists of two parts: the rated-speed analysis and the variable-speed analysis.

At the rated speed, the characteristics of the pump are determined by the relationship between the flow and the head. Therefore, they are obtained according to formula (10) by analyzing and the data fitting. Formula (11) is used to further research its dynamic performance.

$$H_0 = f(Q_0) \tag{10}$$

$$H_0 = f(Q_0) = a + bQ_0 + cQ_0^2 \tag{11}$$

Where:

- $H_0$  ... the rated head,
- $Q_0$  ... the rated flow,
- $a$  ... a constant of more than zero,
- $b$  ... a constant,
- $c$  ... a constant of less than zero.

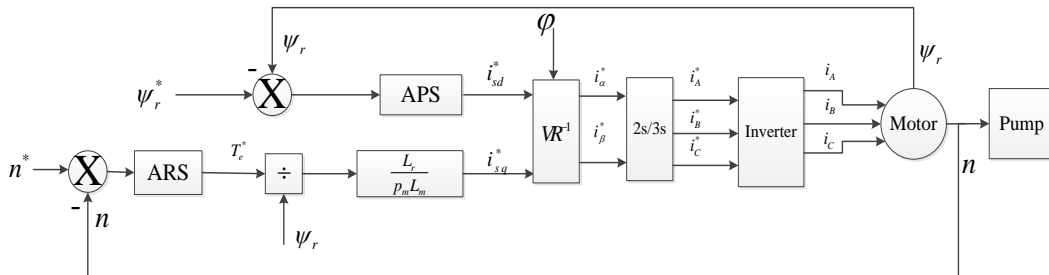


Figure 1. Rotor-flux-oriented vector-control motor model

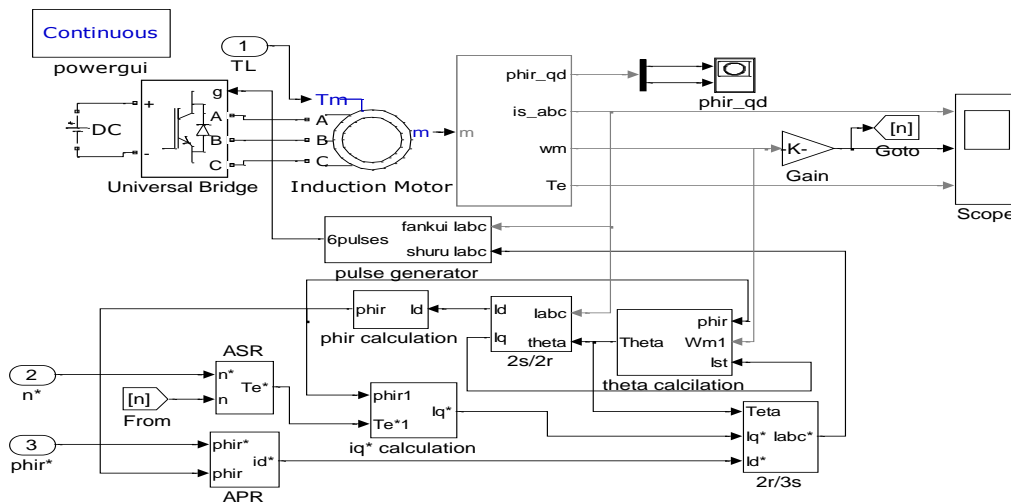


Figure 2. Simulation model of the vector-control system of the induction motor

At a variable speed, the pump characteristics change. According to the similarity theory (affinity laws) of the pump, the characteristic equation of the pump at any speed is [8].

$$\frac{Q}{Q_0} = \frac{n}{n_0} = k \quad (12)$$

$$\frac{H}{H_0} = \left(\frac{n}{n_0}\right)^2 = k^2 \quad (13)$$

$$\frac{P}{P_0} = \left(\frac{n}{n_0}\right)^3 = k^3 \quad (14)$$

Formulas (12) and (13) can be obtained as follows:

$$H = \left(\frac{n}{n_0}\right)^2 f\left(Q \frac{n_0}{n}\right) = k^2 f\left(\frac{Q}{k}\right) \quad (15)$$

Where:

- $P$  ... the shaft power of the pump,
- $P_0$  ... the rated power of the pump,
- $n_0$  ... the rated speed of the pump,
- $k$  ... the ratio of the actual and rated speed.

Formula (15) is the characteristic equation of the pump at any speed. At the rated speed, the characteristic curve of the pump is drawn using the original data as shown with curve 1 in Fig. 3. Curve 2 is the characteristic curve at any speed.

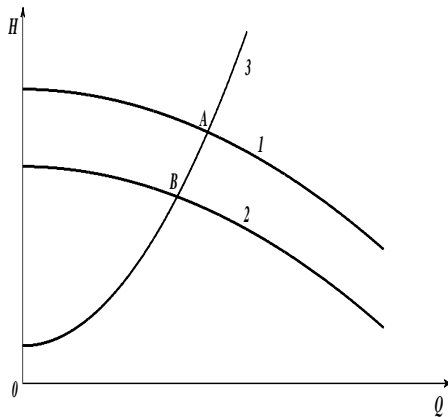


Figure 3. Pump characteristics and pipeline characteristic curve

The pipeline characteristic of the pump is very important for the dynamic model of the centrifugal pump system, because it determines the operating point of the pump. According to the hydraulic law [9], that can get the pump pipeline characteristic equation is [10]:

$$H = H_{st} + SQ^2 \quad (16)$$

$$S = 8\left(\frac{\lambda l}{d} + \sum \xi\right) / (\pi^2 d^4 g) \quad (17)$$

Where:

- $H_{st}$  ... the static head of the centrifugal pump,
- $S$  ... the resistance coefficient of the pipeline,
- $\lambda$  ... the along resistance coefficient,
- $\xi$  ... the local resistance coefficient,
- $l$  ... the length of the pipeline,
- $d$  ... the diameter of the pipeline,
- $g$  ... the gravity acceleration.

According to the pipeline characteristic formula (16), curve 3 can be drawn as shown in Fig. 3. The operating point of the pump is determined by the characteristic of the pump and the characteristic of the pipeline. Curve 3 is intersected with curve 1 and curve 2 at the A and B points respectively in Fig. 3, which are the operating points of the pump at different speeds [11]. However, the position of the operating point is directly related to the efficiency of the pump. The efficiency expression is:

$$\eta = \frac{\rho g H Q}{P} \quad (18)$$

$$P = T_L \frac{2\pi n}{60} \quad (19)$$

Where:

- $\rho$  ... the water density,
- $T_L$  ... the torque load.

According to formula (18), the  $\eta-Q$  curve can be fitted as shown in Fig. 4, to get the best efficiency point M.

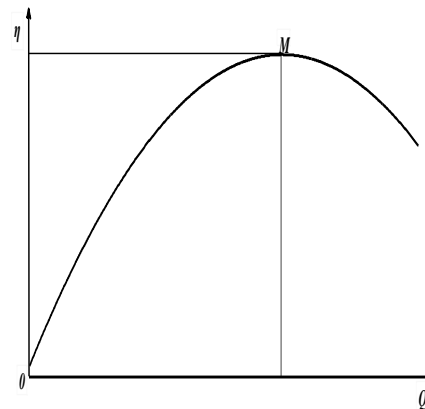


Figure 4. Efficiency curve of the pump

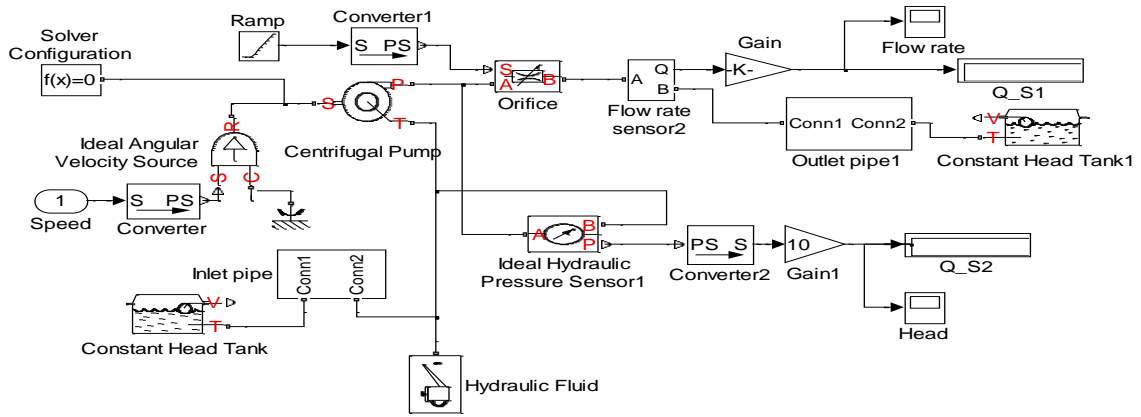


Figure 5. Simulation model of the centrifugal-pump system

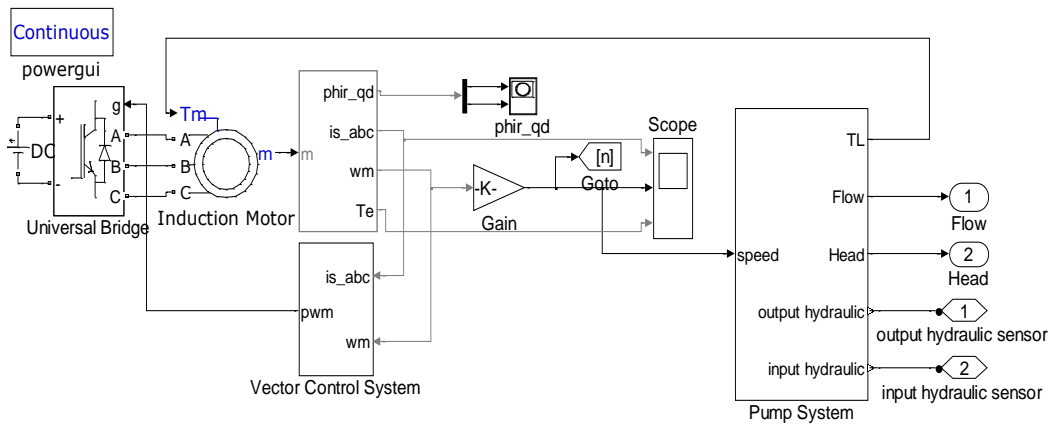


Figure 6. Simulation model of the motor-pump system

When the operating point of the pump is maintained close to the M point, the efficiency of the pump is maximally utilized. It is well known that there are two ways to change the operating point of the pump in Fig. 3. One is to change Curve 3 by adjusting the valve, which decreases the efficiency of the centrifugal pump. The other is to change the position of Curve 2 by adjusting the speed. In the motor-pump system, the latter is used to adjust the speed of the motor by using the vector-control strategy, thus making the pump to operate at a high-efficiency rate. The model simulation of the centrifugal pump is shown in Fig. 5.

#### 4. SIMULATION RESULTS AND ANALYSIS

To analyze the centrifugal pump and three-phase induction motor, the CDL2-8 and YB2-80M2-2 types, respectively, are selected [12]. The rated speed and power of the motor are 2830r/min and 1.1KW, respectively. The rated speed of the pump is 2830r/min. The specific parameters are shown in Tables 2 and 3. The simulation model of the whole motor-pump system is shown in Fig. 6.

Table 2: Parameters of the three-phase induction motor

Parameter	$U / f$	$n_m$	$P_m$	$R_r / R_s$	$L_r / L_s$	$L_m$
Rated value	380V/ 50HZ	2830 r/min	1.1 KW	5.313Ω/ 6.959Ω	0.029H/ 0.029H	0.67 86H

Table 3: Parameters of the centrifugal pump

Parameter	$n_N$	$P_N$	$H$	$Q$
Rated value	2830r/min	1.1KW	67.5m	2.0m <sup>3</sup> /h

The simulation results show that the motor reaches the rated speed of 2830r/min under the rated voltage and load conditions. The rapid response of the system reaches the steady-state at about  $t=0.02s$  (in Fig. 7). When the speed of the motor increases from 0 to 2830 r/min, the electromagnetic and load torque get stable at 3.6N.m and 3N.m, respectively, (Fig. 8). The output speed and torque of the induction motor match the set target of the pump by using the rotor-flux-oriented vector control in Figs. 7 and 8, which provides the basis for the high-efficiency operation of the centrifugal pump.

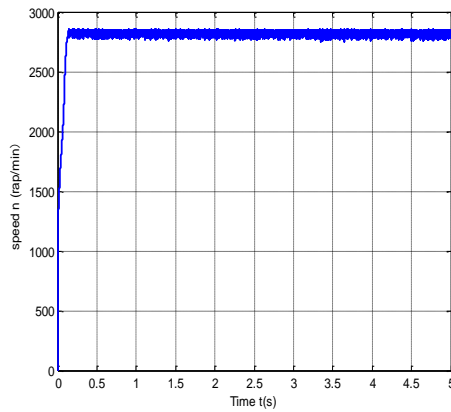


Figure 7. Output speed of the motor

The centrifugal pump and the motor are directly connected through the rotating shaft. The output speed and the output power of the rotating shaft are the input speed and shaft power of the centrifugal pump, respectively, and the torque is used to drive the centrifugal pump load. When the pump input speed is increased from 0 to 2830r/min, the curve of the flow and the head increase, respectively, as shown in Fig. 9. The output flow rate is zero at  $t=0-0.01s$ , as determined by the pipeline characteristic of the pump. The pump head is more than the static head; it is 15m at  $t=0.01s$ . The flow begins to output at the pump outlet. The head quickly reaches the maximum value of 83.50m at  $t=0.04s$ . Subsequently, the flow gradually increases to  $3.55m^3/h$ , and the head decreases until reaching stability of 32m.

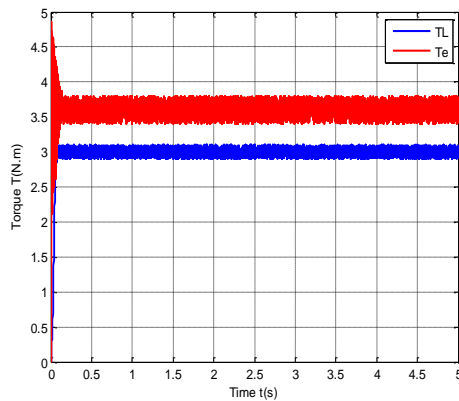


Figure 8. Electromagnetic torque and load torque

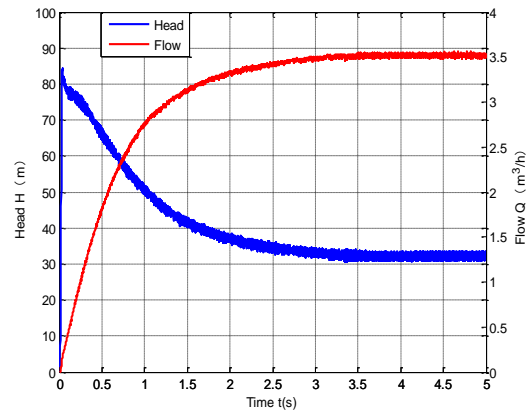


Figure 9. Pump output flow and head at the rated-speed

For the efficiency of the centrifugal pump to be mainly related to the head, flow and shaft power, formula (18) should simply be used. The expressions for the head and shaft power are obtained with the flow based on the similarity law. The efficiency and the flow implement the following quadratic fit:  $n = -8.576 * q^2 + 38.972 * q + 6.5588$ . Derivation of the above expression  $\frac{dn}{dq} = 0$  yields  $q = 2.27$  with the second derivative  $\frac{d^2n}{dq^2} < 0$ , the efficiency reaches the maximum value of 50.83% of the flow rate of  $2.27m^3/h$ .

According to formula (18), could be obtained the efficiency curve is attained based on the head and the flow output waveform as shown in Fig. 10. At the time  $t=0.7s$ , the efficiency reaches the maximum value of 50.80%. The corresponding flow of the pump is about  $2.4m^3/h$ , and the head is close to 55m. The simulation results are very close to the theoretical results, thus indicating the validity and stability of the system model. In engineering, the high-efficiency rate of the pump operation is the maximum efficiency of the pump decrease in the range from 5% to 8% [13]. According to the calculated of 8%, the high-efficiency rate of the pump is in the range from 46.7% to 50.80%.

The controlled speed of the motor can control the rate of the pump output flow, while the flow rate is directly related to the efficiency of the centrifugal pump. The rotor-field-oriented vector-control strategy is adopted to control the output speed of the motor in order to analyze the efficiency of the centrifugal pump. At the motor output speed in the range from 2830r/min to 2700r/min, every band declines to 100r/min until 1800r/min and finally rises to 2830r/min (Fig. 12). There is a total of twelve bands. As shown in Fig. 9, for the flow and head to reach a steady-state, it takes about 5s at the rated speed, so the sampling time of each speed band is 5s.

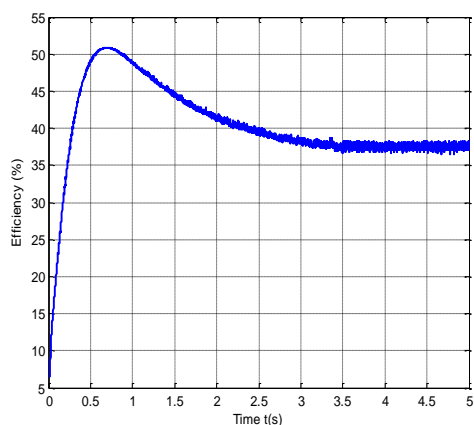


Figure 10. Efficiency of the centrifugal pump

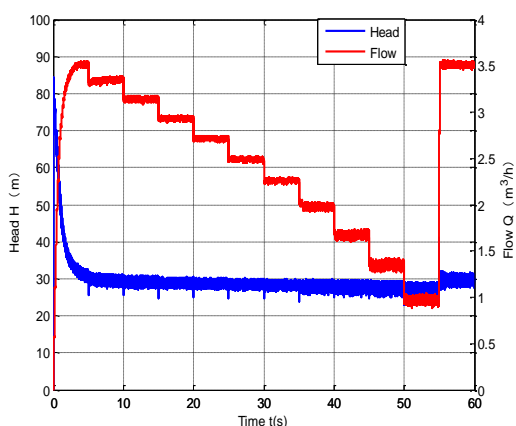


Figure 11. Head and flow output of the pump at a variable speed

According to the characteristics of the pump, the flow and head output change at a variable speed. The flow and head output of the centrifugal pump are shown in Fig. 11. The response and steady-state can be fast at the speed jump time. The efficiency curve of the centrifugal pump is obtained as shown in Fig. 12. At the beginning, the speed decrease corresponds to the increase in the pump efficiency. When the speed reaches 2200r/min, the pump efficiency is at its maximum value of 50.80%. Thereafter, the efficiency of the pump gradually decreases with the speed decrease. At the pump high-efficiency rate in the range from 46.74% to 50.80%, the corresponding centrifugal pump operates in the range from 2000r/min to 2500r/min. As shown in Figs. 11 and 12, when the efficiency of the centrifugal pump reaches the maximum value of 50.80%, the corresponding flow rate is  $2.3\text{m}^3/\text{h}$ , which is very close to the theoretical value of  $2.27\text{m}^3/\text{h}$ .

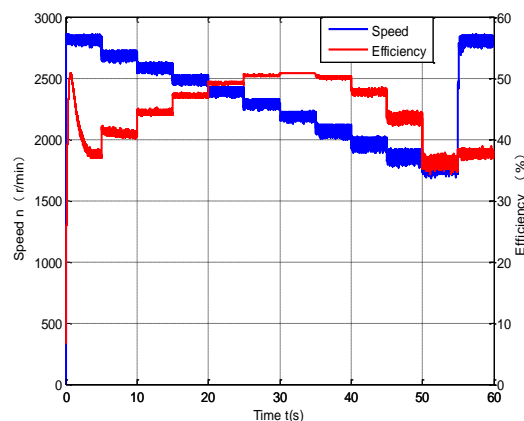


Figure 12. Output efficiency at a variable speed

## 5. CONCLUSION

In this paper, a rotor-flux vector-control strategy is used to analyze the dynamic property of the induction-motor centrifugal-pump system under variable rotation-speed conditions. The simulation results show the accuracy and stability of the rotor-field-oriented vector-control strategy. The efficiency of the centrifugal pump is analyzed, and the speed of the centrifugal pump operation at a high-efficiency rate is in the range from 2000r/min to 2500r/min. The attained results provide the reference values for further research towards improvement of the efficiency of the motor-pump system.

## ACKNOWLEDGMENTS

This work was financed by the National Science and Technology Support Project of China (2013BAF01B02), the Young Core Teacher Program of the Anhui University (J01005126), and the Academic and Technology Leaders Imported Project of the Anhui University (02303203(32030049)). The authors gratefully acknowledge HENG DA JIANG HAI Co. Ltd. for their work on the hydraulic-characteristics test.

## REFERENCES

- [1] Liu Hong, Zhai Qingzhi., "Simulation study on irrigation system with variable frequency drive of water pump", *Journal of China Agricultural University*, 19 (6), pp. 201-207, 2014.
- [2] Shi Fengxia, Yang Junhui, Wang Xiaohui, "Effect of rotating speed on hydraulic energy recovery turbines performance", *2013 ACMS. Applied Mechanics and Materials*. 444-445. pp. 1033-1037, 2014.
- [3] Yang Hongyan, Hu Gejin, "Compare the Dynamic Characteristics of Inlet and Outlet Throttle Speed-Regulating Hydraulic System", *2011 ICMSET. Advanced Materials Research*, Zhengzhou, China, 462, pp. 833-838, 2011.
- [4] M.I. Jahmeerbacus, "Flux Vector Control of an Induction Motor Drive for Energy-efficient Operation of a Centrifugal Pump", *Proc. 2015 IEEE Industrial Engineering and Operations Management*, Dubai, United Arab Emirates, pp. 33-35, 2015.

- [5] Rashed, Mohamed, MacConnell, Peter F. A, Stronach, A. Fraser, Acarnley, Paul, "Sensorless indirect-rotor-field-orientation speed control of a permanent-magnet synchronous motor with stator-resistance estimation", *Automation & Control Systems*, 54(3), pp. 1664-1675, 2007.
- [6] E.Bortoni, R.Almeida, A.Viana, "Optimization of parallel variable speed driven centrifugal pumps operation", *Energy Effic*, 1(3), pp. 167-173, 2008.
- [7] F.J.T.E.Ferreira, J.A.C.Fong and de A.T.Almeida, "Ecoanalysis of variable-speed-drives for flow regulation in pumping systems", *IEEE Transactions on Industrial Electronics*, 58(6), pp. 2117-2125, 2011.
- [8] Simpson, Angus R, Marchi, Angela, "Evaluating the Approximation of the Affinity Laws and Improving the Efficiency Estimate for Variable Speed Pumps". *Engineering Mechanical*, 139(12), pp. 1314-1317, 2013.
- [9] Kelemen, Katharina, Schuch, Anna C, Schuchmann, Heike P, "Influence of Flow Conditions in High-Pressure Orifices on Droplet Disruption of Oil-in-Water Emulsions", *CHEMICAL ENGINEERING & TECHNOLOGY*, 37(7), pp. 1227-1234, 2014.
- [10] Handong Wang, "Water flow rate models based on the pipe resistance and pressure difference in multiple parallel chiller systems", *Energy and Buildings*, 75, pp. 181-188, 2014.
- [11] T.Ahonen, J.Tamminen, J.Ahola, J.Viholainen, " Estimation of pump operational state with model based methods", *Energy Convers.Manag.*, 51(6), pp. 1319-1325, 2015.
- [12] W.V. Jones, "Motor selection for centrifugal pump applications made easy", *Proc. 2011 IEEE Pulp and Paper Industry Technical Conference (PPIC)*, Nashville, TN, United States, pp.140-150, 2011.
- [13] Qinghui Wu, Xinjun Wang, Qinghuan Shen, "Research on dynamic modeling and simulation of axial-flow pumping", *Neurocomputing*, 186, pp. 200-206, 2016.

**Xiwen Guo** received his B.Sc. and M.Sc. degrees in Power Electronics & Power Drive from the Anhui University of Science & Technology in 2005 and 2008, respectively, and his Ph.D. degree in Electrical Engineering from the Hefei University of Technology in 2012. Since 2012, he has been a Lecturer with the School of Electrical Engineering and Automation of the Anhui University of China. His current research interests include design and analysis of the novel spherical actuator and its control, power electronics & power drive, and motor-pump modeling.

**Yuliang Wu** graduated from the Chuzhou University of China in 2015. He is currently working towards his M.Sc. degree at the School of Electrical Engineering and Automation of the Anhui University of China. His research interests include efficient coupling of the motor and pump.

**Guoli Li** received her Ph.D. degree in electrical engineering from ASIPP, Hefei, China, in 2008. Currently, she is a professor of the School of Electrical Engineering and Automation of the Anhui University of China. Her interest is in electrical & electronic engineering and intelligent optimization techniques.

**Chao Lu** graduated from the Anhui University of China in 2014. He is currently working towards his M.Sc. degree at the School of Electrical Engineering and Automation of the Anhui University of China. His research interests include intelligent optimization techniques and motor-pump modeling.